Supplementary Information

Hybrid organic-inorganic polyoxovanadates with $[M(en)_n]$ (M=Co, Ni, Cu, Zn) displaying (V_4O_{13}), ($V_{15}O_{36}$) or ($V_{18}O_{42}$) morphologies

Emilie Skytte Vosegaard,[a] Mohammad Aref Hasen Mamakhel[a] and Bo Brummerstedt Iversen*[a]

[a]Center for Sustainable Energy Materials, Department of Chemistry, Aarhus University, Langelandsgade 140, 8000 Aarhus C, Denmark.

*Correspondence e-mail: bo@chem.au.dk

S1 Sample quality

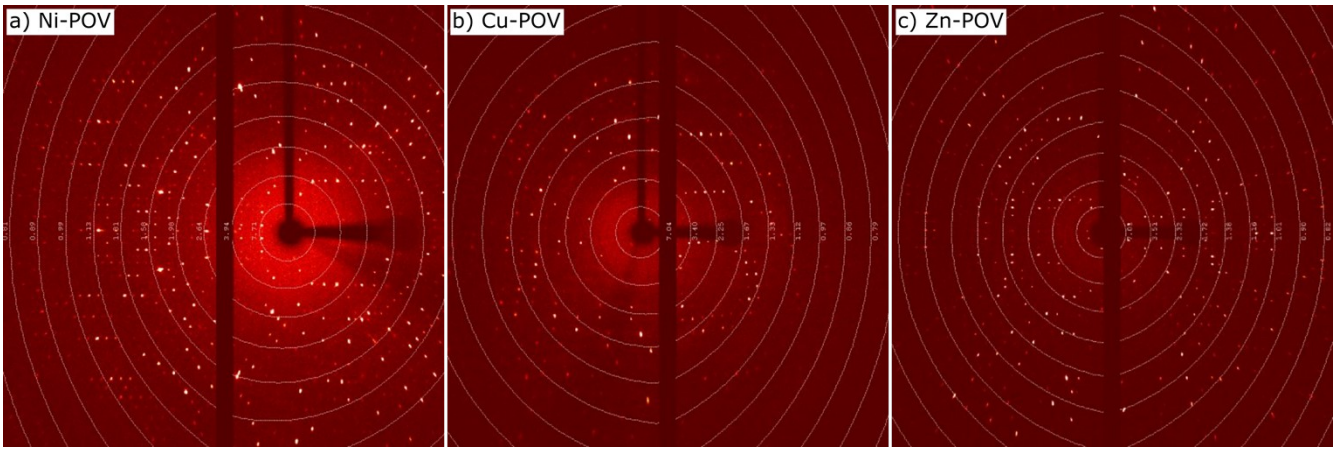

Figure S1: Detector frames showing scattering from the a) Ni-, b) Cu- and c) Zn-POV structures.

The black Ni-POV crystals formed rounded obelisk shapes grown from a central grain resulting in star shaped multicrystals (Figure 1b). Cutting one limb from the star gave an intrinsically twinned crystal with low long-range order/high mosaicity as evident from 1) a large scattering footprint on the detector and 2) an unexpectedly low angular resolution despite low experimental temperature and high exposure time (360 s/frame) (Figure S1a). Due to the large direct space unit cell, contracting the reciprocal lattice, proper peak separation of twin components required a longer detector distance of 52 mm. Attempts to recrystallize the Ni-POV sample unsuccessfully resulted in clear transparent crystals of ethylenediammonium dichloride. Taking the poor crystal quality into account, acceptable reliability factors were obtained for the structure solution: R_{int}=8.2%, R(F^2)=9.7% and *w*R(F^2)=27.2% (Table 1). Reasonably low residuals were obtained by placing O atoms on Q-peaks in the voids, as evidence of crystal water occupying the empty void space. H atoms could not be resolved in the structure, but were assumed in the chemical formula for charge neutrality. Ligand en geometry and ADPs were modelled using SHELX constraints when needed.

Cu-POV forms feather shaped plates of twinned crystals (Figure 1c), with similar problems as the Ni-POV sample, despite the smaller unit cell making it possible to use the preferred detector distance of 40 mm (Figure S1b). The similar *a* and *c* parameters, along with twinning and high mosaicity in the crystals, created an apparent tetragonal supergroup P*4/nnc*, with a maximal invariant subgroup relation to the P*nn2* space group reported here. R-factors of similar quality to Ni-POV were obtained R_{int}=9.2%, R(F^2)=6.8% and *w*R(F^2)=18.6% (Table 1), and similar precautions regarding H atoms and en geometry had to be taken for a physical structure solution.

The Zn-POV sample formed block shaped crystals of high quality (Figure 1d), as evident from the intense, well separated diffraction (Figure S1c) and good quality parameters R_{int}=3.6%, R(F^2)=3.9% and *w*R(F^2)=10.3% (Table 1). This allowed for a full structure solution and unconstrained ADP refinement of all atoms heavier than H, which were assumed riding. Disorder of one of the en groups was handled by split sites.

Attempts to crystallize products from the substrate of the Ni, Cu and Zn synthesis, akin to how Co-POV was formed, immediately revealed discrepancies, as substrate color varied from clear red for the Co synthesis over black for Ni and dark blue/purple for Cu to clear green for Zn. Black crystals were successfully formed in the Ni and Cu substrate, while the Zn substrate did not crystallize. A structure of poor quality very similar to Ni-POV was formed from the Ni substrate, however crystallizing in the cubic P*a-3* space group (*a*=34.14721(18) Å). Cu-POV crystals were formed in the Cu substrate, although poor crystal quality only allowed for a poor structure solution in the tetragonal P*4/nnc* (*a*=14.6801(3) Å, *b*=18.6315(10) Å) supergroup of the actual Cu-POV P*nn2* space group.

S2 Powder X-ray diffraction

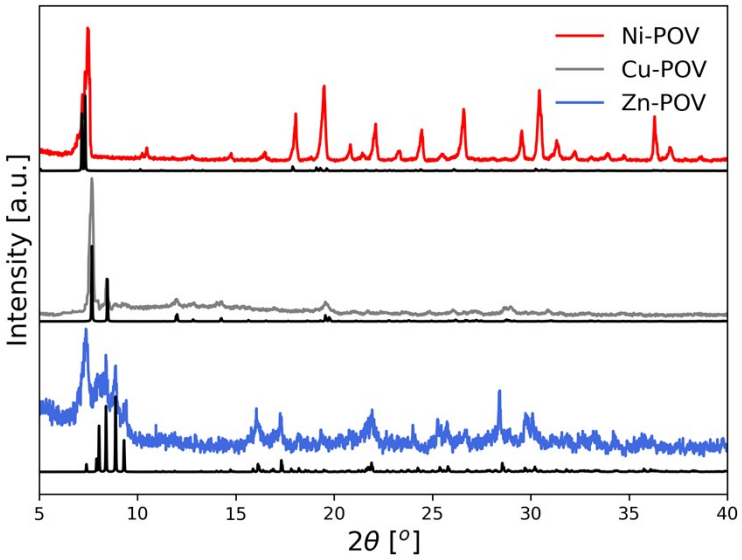

Figure S2: PXRD of the Ni-, Cu-, and Zn-POV samples measured with Cu Kα radiation at 300 K. Black overlays are the diffractograms simulated from the SCXRD structure. Discrepancies between PXRD and SCXRD are explained

by experimental deviations e.g. temperature differences (peak position) and poor powder average (peak intensity).

Due to the large unit cell parameters a high number of peaks are observed in the diffraction patterns. This combined with the high absorption of the sample at the used wavelength, along with asymmetric peak shape due to instrumental features, results in a noisy diffractogram with large peak overlap. These conditions are not ideal for detection of minor impurity phases, but allows us to identify the reported structures as the major product, if not the only product. The different experimental temperatures for PXRD (room temperature) and SCXRD (100 K or 150 K) results in a small shift in peak position. Relative peak intensities may vary due to poor powder average (break down of the assumption of perfectly random orientation of crystallites) since preferred orientations may occur in the sample of relatively large single crystals (Figure S1).

S3 Inductively Coupled Plasma

Table S1: Results of ICP analysis for M-POV samples, where M=Cu, Ni, Zn. Values in the main text are calculated from this, with uncertainties estimated from the propagation law.

Sample	V, mg/Kg	Ni, mg/Kg	Cu, mg/Kg	Zn, mg/Kg
NiV-4-18	31.30	7.50	-	-
Std. dev.	0.69	0.07		
CuV-4-18	97.10	-	26.92	-
Std. dev.	0.96		0.23	
ZnV-2-15	73.70	-	-	13.10
Std. dev.	0.09			0.03

S4 Fourier Transform Infrared Spectroscopy

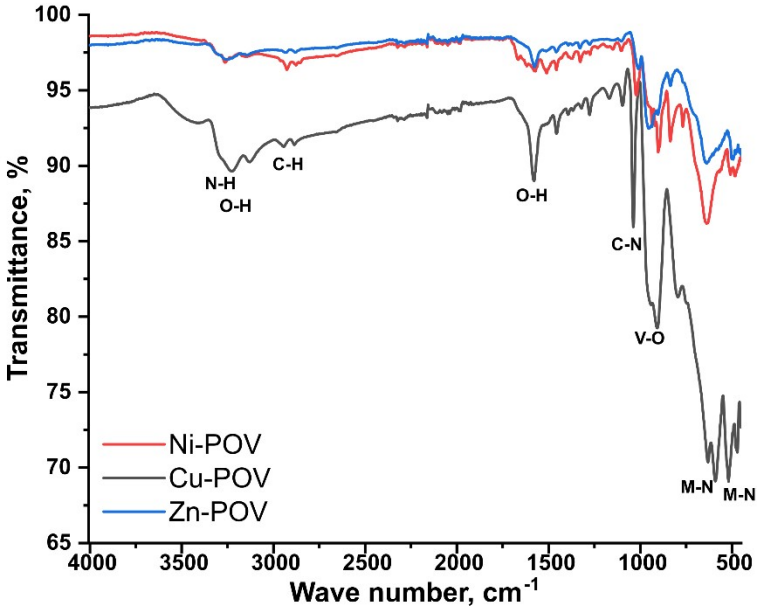

Figure S3: FTIR spectra of the Ni-, Cu-, and Zn-POV samples.

In the FT-IR spectrum of Figure S7, we assume that bands >3000 cm^{-1} assign to N-H (amine stretching) and O-H (water stretching), while C-H related absorption bands are seen just below 3000 cm^{-1}. Absorption peaks at 1580 cm^{-1}, 1037 cm^{-1} and 800 cm^{-1} are characteristic for O-H (water bending), C-N and N-H (amine bending), respectively. The sharp band just below 1000 cm^{-1} is characteristic for the V-O stretching mode of the terminal V-O group. The intense peaks around 500-700 cm^{-1} are characteristic for metal-N bonds.

To test stability, we measured the IR spectra of the freshly synthesized complexes and repeated them seven months later. The results show that these complexes are stable at room temperature. But they are not heat-resistant, meaning they decompose when heated. This is a very common occurrence for complex compounds. Here, the FT-IR spectra of Ni-POV, Cu-POV and Zn-POV are shown.

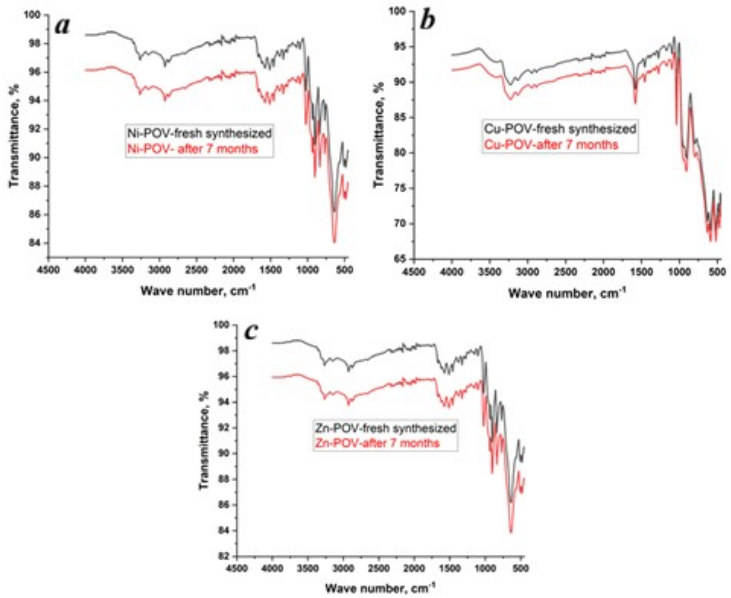

Figure S4: FTIR spectra of the Ni-POV (a), Cu-POV (b), and Zn-POV (c) as fresh prepared samples and after 7 months.

S5 UV-vis

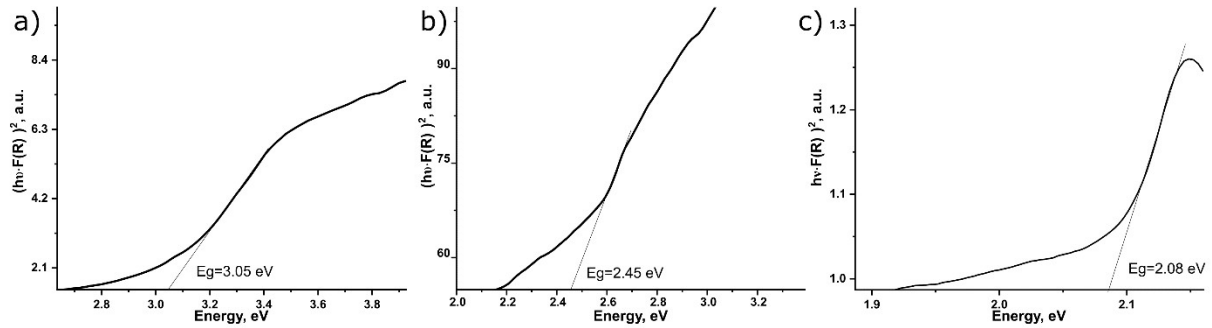

Figure S5: Direct band gap energies of a) Ni-, b) Cu-, and c) Zn-POV.

S6 Crystal structures

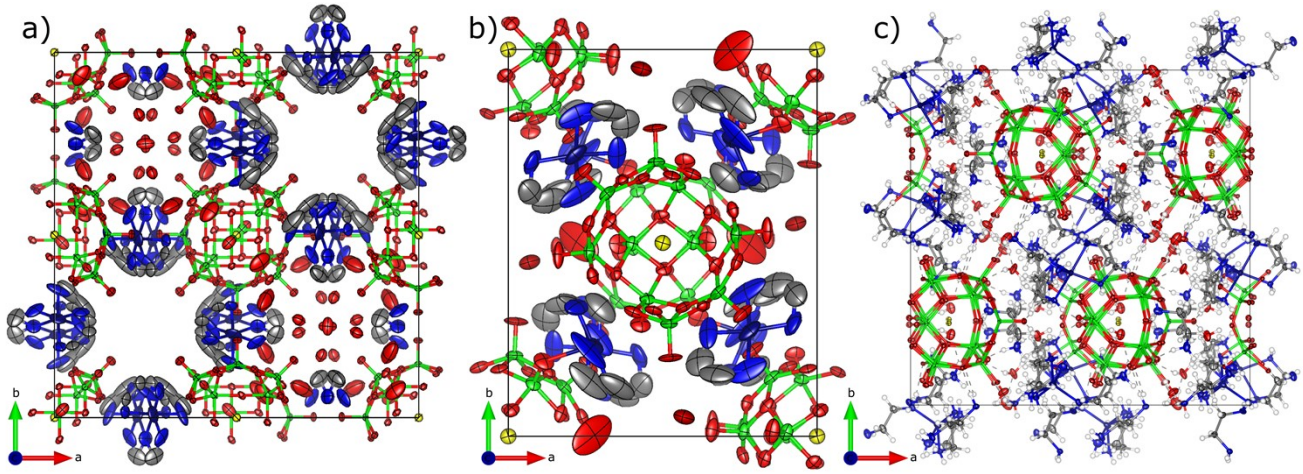

Figure S6: SCXRD structure with ADPs of a) Ni-, b) Cu-, and c) Zn-POV.

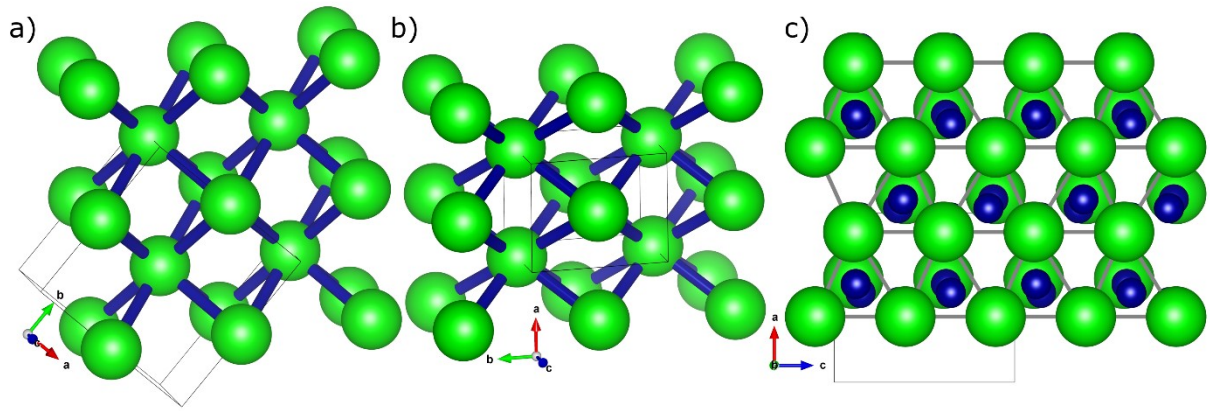

Figure S7: Framework diagrams of a) Ni-, b) Cu-, and c) Zn-POV. Green spheres represent the POVs and blue lines indicate [Ni(en)$_3$] or [Cu(en)$_2$] complexes linking the POVs in a) and b). Meanwhile in c), [Zn(en)$_2$(enH)] is shown as blue spheres, occupying the tetrahedral interstitial sites, and gray lines are used to indicate shortest POV contacts, highlighting the hexagonal arrangement.

S7 Elemental analysis

The calculated mass percentages of C, H, N in the formulas of Cu-POV, Ni-POV, Zn-POV and the experimentally measured values are in good agreement. The table shows experimentally measured mass % of C, H, N in crystals and these results confirm the veracity.

Table S2: Results of CHN analysis for M-POV samples, where M=Cu, Ni, Zn.

Compound	N, mass%	C, mass%	H, mass%
Cu-POV	9.2	7.9	3.0
Ni-POV	11.9	10.2	4.4
Zn-POV	9.6	8.3	3.6

In Tables S3, S4 and S5 we present the experimental and theoretical values side by side. The obtained results can be used with confidence to determine the molar ratio of M/V, where M=Ni, Cu, Zn.

Comparison of the calculated and experimental data of the molar ratio M/V and mass percentages of C, H, N. show, they agree well and there are no significant discrepancies.

Table S3: 4[Ni(en)$_3$]·(V$_{18}$O$_{42}$Cl)·13.25(H$_2$O)

Element	Calculted, mass%	Calculated Mol ratio of Ni/V	Measured, by ICP and CHN analysis	Measured Mol ratio of Ni/V
Ni	8.33	0.22	7.50 ppm	0.21
V	32.52		31.3 ppm	
C	10.22		10.2 mass%	
H	4.38		4.4 mass%	
N	11.92		11.9 mass%	

Cl	1.25		-	
O	31.36		-	
Total	100			

Table S4: $4[Cu(en)_2]\cdot(V_{18}O_{42}Cl)\cdot 4(H_2O)$

Element	Calculted, mass%	Calculated Mol ratio of Cu/V	Measured, by ICP and CHN anaysis	Measured Mol ratio of Cu/V
Cu	10.455	0.22	36.92 ppm	0.22
V	37.713		97.10 ppm	
C	7.904		7.9 mass%	
H	2.985		3.0 mass%	
N	9.217		9.2 mass%	
Cl	1.458		-	
O	30.268		-	
Total	100		-	

Table S5: $2[Zn(en)_2(enH)]\cdot(V_{15}O_{36}Cl)\cdot(enH_2)\cdot 5.63(H_2O)$

Element	Calculted, mass%	Calculated Mol ratio of Zn/V	Measured by ICP	Measured Mol ratio of Zn/V
Zn	6.413	0.13	13.1 ppm	0.13
V	37.472		73.7 ppm	
C	8.246		8.3 mass%	
H	3.559		3.6 mass%	
N	9.617		9.6 mass%	
Cl	1.738		-	
O	32.954		-	
Total	100		-	

S8 Thermogravimetric analysis

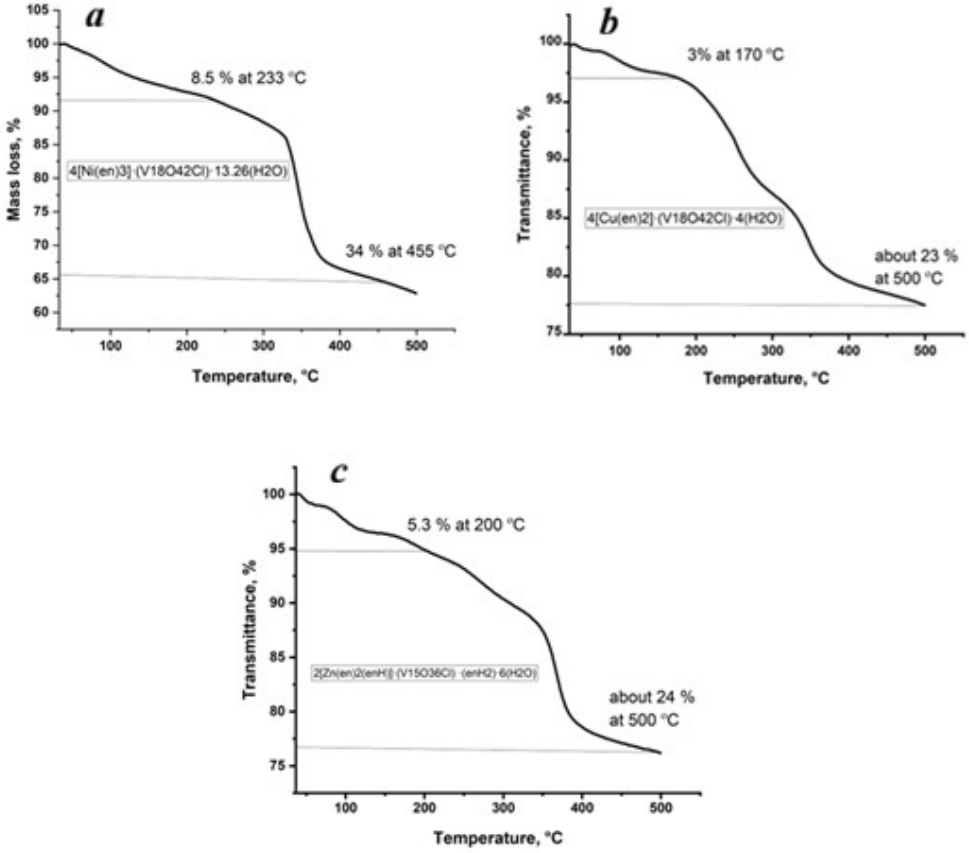

Figure S8. TGA of the Ni-POV (a), Cu-POV (b), and Zn-POV (c) samples

The results of thermogravimetric analysis (TGA) are shown above. TGA shows water contents of approximately 8.5%, 3%, and 5.3% in the Ni-POV, Cu-POV, and Zn-POV samples, respectively.

The TGA of Ni-POV (a), Cu-POV (b) and Zn-POV (c) also show mass loss of organic molecules approximately 34%, 23% and 24% respectively. These TGA results are in good agreement with the content of water and organic molecules of the structures as obtained from SCXRD. The structures found by SCXRD contain 8.46%, 2.96% and 4.97% water and 34.85%, 23.36% and 26.45% organic molecules for Ni-, Cu- and Zn-POV, respectively.

S9 EPR

We have measured EPR spectra of all three samples, and Cu-POV and Ni-POV have clear signals showing that some elements have unpaired electrons. $Cu^{2+}(3d^9)$, $V^{4+}(3d^1)$, and $Ni^{2+}(3d^8)$ are paramagnetic, but $Zn^{2+}(3d^{10})$ and $V^{5+}(3d^0)$ are diamagnetic.

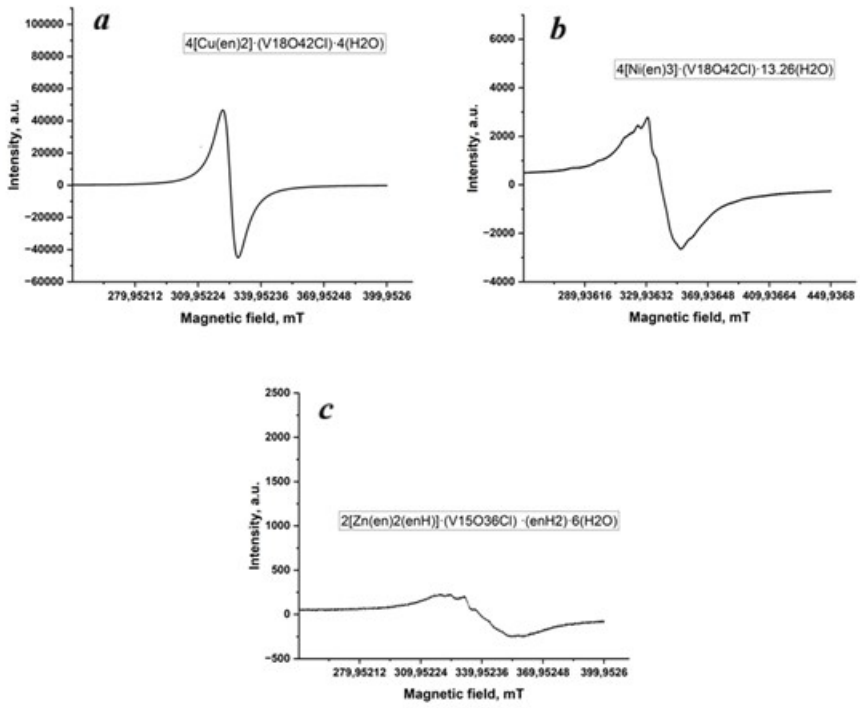

Figure S9. EPR spectra of a) Cu-POV-, b) Ni-POV, and c) Zn-POV.